

RESEARCH ARTICLE

Historical and projected climate change over three major river basins in China from Fifth and Sixth Coupled Model Intercomparison Project models

Xian Zhu^{1,2,3}  | Zhenming Ji^{1,2,3} | Xiaohang Wen⁴ | Shao-Yi Lee^{1,2,3} |
Zhigang Wei⁵  | Zhiyuan Zheng^{1,2,3} | Wenjie Dong^{1,2,3}

¹School of Atmospheric Sciences, Sun Yat-Sen University, Zhuhai, China

²Key Laboratory of Tropical Atmosphere-Ocean System, Ministry of Education, Zhuhai, China

³Southern Marine Science and Engineering Guangdong Laboratory, Zhuhai, China

⁴Plateau Atmosphere and Environment Key Laboratory of Sichuan Province, School of Atmospheric Sciences, Chengdu University of Information Technology, Chengdu, China

⁵State Key Laboratory of Earth Surface Processes and Resource Ecology, Faculty of Geographical Science, Beijing Normal University, Beijing, China

Correspondence

Xiaohang Wen, Plateau Atmosphere and Environment Key Laboratory of Sichuan Province, School of Atmospheric Sciences, Chengdu University of Information Technology, Chengdu 610225, China.
Email: wxh@cuit.edu.cn

Wenjie Dong, School of Atmospheric Sciences, Sun Yat-Sen University, Zhuhai 519082, China.
Email: dongwj3@mail.sysu.edu.cn

Funding information

National Key R&D Program of China, Grant/Award Number: 2016YFA0602703; Sun Yat-Sen University, Grant/Award Number: 19lgpy31; China Postdoctoral Science Foundation, Grant/Award Number: 2020M672942; Strategic Priority Research Program of Chinese Academy of Sciences, Grant/Award Number: XDA20060401

Abstract

When assessing the socio-economic impacts of climate change, it is sensible to make targeted climate projections for regions of high population density and economy activity. Much of human activity is concentrated at river basins, yet it has been difficult to resolve the complex boundaries of these basins in coarse resolution global climate models. The latest high-resolution observation and climate projection datasets enable such basin-based evaluations now, and this study assesses the historical and projected climate changes over three major river basins in China—the Yellow, Yangtze and Pearl River basins. Based on CN05.1 dataset, the Yellow River basin has significantly warmed by about 1.8°C over the past five decades, far more than the other two basins. The change in temperature extremes has been as severe, with the annual maxima of daily maximum temperatures (TXx) increasing by 1.5°C, and the annual minima of daily minimum temperatures (TNn) increasing by 2.5°C. Precipitation over the Yangtze River has significantly increased by about 0.2 mm·day⁻¹, while changes over the other two basins were not statistically significant. The uncertainty in the change of precipitation was greater than that of temperature. A selection of simulations from the Fifth and Sixth Coupled Model Intercomparison Projects (CMIP5 and CMIP6) were validated against the CN05.1 dataset for the historical period of 1961–2018. Changes in temperature indices were well-reproduced, but changes in precipitation indices poorly so. CMIP6 models performed better than the CMIP5 models. Both CMIP5 and CMIP6 multi-model ensembles (MMEs) projected about 1.0–2.0°C warming over China and the three river basins by 2015–2050. Both MMEs projected wetting trends over most parts of China and the three river basins. Both warming and wetting were projected to accelerate with time, particularly warming over the Yellow River basin, and wetting over the Pearl River basin.

KEYWORDS

climate change, CMIP5, CMIP6, projection, river basins

1 | INTRODUCTION

Global climate change has attracted worldwide attention in the recent decades (Kurane, 2010; Tian *et al.*, 2016). In particular, changes in regional temperature and precipitation can result in significant socio-economic impacts (Piao *et al.*, 2014; Yu *et al.*, 2014; Wang *et al.*, 2017). Therefore, it is essential to evaluate temperature and precipitation changes at regional spatiotemporal scales.

Climate change over China will potentially impact the largest population in the world. At the same time, climate projections for China are challenging due to the diverse regional climates inside its borders (Li *et al.*, 2018). Most parts of China have experienced significant warming over the period of 1955–2012 (Jin *et al.*, 2015). Generally, the warming has been stronger over the north compared to the south, but there remain large differences in regional trends (Ge *et al.*, 2013). The country's population and gross domestic product (GDP) production is concentrated over three regions, which national planning typically focuses on. These are the enormous catchment basins of the Yellow, Yangtze, and Pearl Rivers, along river lengths of 5,464, 6,300 and 2,320-km, and covering areas of 752,443, 1,800,000 and 440,000 km², respectively (Zhao *et al.*, 2011). The Yangtze and Pearl Rivers have the highest discharges in China, as well as the highest frequencies of flooding in last several decades (Yang *et al.*, 2015; Su and Chen, 2019).

There has been significant ecological and environmental damage in the three river basins over the last 30 years. While this was in part to rapid development (Peng *et al.*, 2017; Omer *et al.*, 2019), climate change and its impact on hydrological processes has also exacerbated the situation, for example, accelerated glacial retreat at the sources of the Yellow and Yangtze Rivers (Bao and Feng, 2016). Climate change may affect the frequency, size, location and duration of hydrological extreme events (Tang *et al.*, 2017; Wang *et al.*, 2018; Wu *et al.*, 2018), and increased extreme events in China often result in greater impacts compared to increases of the mean state (Xu *et al.*, 2019). Hence, climate change over the river basins has aroused great concern amongst local scientists (Xi *et al.*, 2018; Xu *et al.*, 2019).

Multiple studies of climate change over different river basins in China have been carried out in recent years. Most studies were either based on coarse-resolution earth system models (Sun *et al.*, 2015; Xu *et al.*, 2019) or did not differentiate between river basins in different geographical regions (Bao *et al.*, 2015; Bao and Feng, 2016). Both observation and model data available in past were low resolution, and not ideal for analysing climate change over geographically complex river basins. This limitation has been overcome with the availability of

high-resolution data from the sixth phase of the Coupled Model Intercomparison Project (CMIP6) and High-Resolution Model Intercomparison Project (HighResMIP; Haarsma *et al.*, 2016). Recent assessment of HighResMIP results found that the increased spatial resolution improves model simulation of rainfall in tropical cyclones (Zhang *et al.*, 2021). Otherwise, the HighResMIP still not widely used for regional climate change projections over China.

This study fills in the abovementioned gaps of previous studies by using output from high-resolution simulations, updating climate projections with CMIP6, and studying three individual river basins with geographical climates. Historical and projected changes in three temperature and three precipitation indices over the Yellow, Yangtze and Pearl River basins are presented below. The article is structured as follows: Section 2 introduces the data, and methods used in the study; section 3 evaluates observed and simulated historical climate change, followed by projected climate change; section 4 presents the conclusions of the study and discusses some questions that arose in the study.

2 | DATA AND METHODS

2.1 | Observation and model outputs

The gridded observation-based dataset CN05.1 was used for calculating historical climate change and validating model performance (Xu *et al.*, 2009; Wu and Gao, 2013). This dataset consists of monthly and daily temperature and precipitation from the period of 1961–2018 and is based on observations from 2,416 stations interpolated to the horizontal resolution of $0.25 \times 0.25^\circ$.

In this study, eight models participating in the Historical and RCP8.5 Experiments of the Fifth Coupled Model Intercomparison Project (CMIP5) (Taylor *et al.*, 2012) and eight models participating in the High-Resolution Model Intercomparison Project (HighResMIP) of the Sixth Coupled Model Intercomparison Project (CMIP6) were used. Information on the 16 models is provided in Table 1, and more details can be found at <https://esgf-node.llnl.gov/>. The HighResMIP was designed to investigate the impact of horizontal resolution on model bias and simulated climate variability (Haarsma *et al.*, 2016). Model outputs were re-gridded to the $0.25 \times 0.25^\circ$ horizontal resolution of CN05.1 using bilinear interpolation.

The CN05.1 period of 1961–2018 was used to benchmark historical climate changes, against which the 16 models were verified. For climate projections, the period of 1995–2014 was used as the baseline, against which the period of 2021–2035 was compared. The period

TABLE 1 CMIP5 and CMIP6 model descriptions

Model name	Modelling centre (or group)	Experiment	Ensemble	Resolution lat × lon	Atmos_model	Ocean_model	Land_model
BCC-CSM1.1	Beijing climate Center, China Meteorological Administration, China	Historical/RCP8.5	r1i1p1	64 × 128	BCC-AGCM2.1	MOM4_L40v1	BCC_AVIM1.0
BNU-ESM	College of Global change and Earth System Science, Beijing Normal University	Historical/RCP8.5	r1i1p1	64 × 128	CAM3.5	MOM4p1	CoLM+BNUDGVM(C/N)
CanESM2	Canadian Centre for Climate Modelling and Analysis	Historical/RCP8.5	r1i1p1	64 × 128	CanCM4	CMOC	CTEM
CCSM4	National Center for Atmospheric Research, USA	Historical/RCP8.5	r1i1p1	192 × 288	CAM4	SOM	CLM4
CNRM-CM5	National Centre for Meteorological Research, France	Historical/RCP8.5	r1i1p1	128 × 256	ARPEGE-Climat(v5.2)	NEMO (v3.2)	ISBA
EC-EARTH	EC-Earth consortium, Swedish Meteorological and Hydrological Institute, Sweden	Historical/RCP8.5	r1i1p1	160 × 320	IFS	NEMO	H-TESEL
FGOALS-g2	Institute of Atmospheric Physics, Chinese Academy of Sciences, China	Historical/RCP8.5	r1i1p1	60 × 128	GAMIL2	LICOM2	CLM3
MRI-CGCM3	Meteorological Research Institute, Japan	Historical/RCP8.5	r1i1p1	160 × 320	MRI-AGCM3	MRI-COM3	HAL
CNRM-CM6-1	National Centre for Meteorological Research, France	HighResMIP	r1i1p1f2	128 × 256	ARPEGE-Climat (v6.3)	NEMO (v3.6)	ISBA-CTRIP
CNRM-CM6-1-HR	National Centre for Meteorological Research, France	HighResMIP	r1i1p1f2	128 × 256	ARPEGE-Climat (v6.3.2)	NEMO (v3.6)	ISBA-CTRIP
EC-Earth3P	EC-Earth consortium, Swedish Meteorological and Hydrological Institute, Sweden	HighResMIP	r1i1p2f1	256 × 512	IFS	NEMO (ORCA1)	H-TESEL
EC-Earth3P-HR	EC-Earth consortium, Swedish Meteorological and Hydrological Institute, Sweden	HighResMIP	r1i1p2f1	512 × 1,024	IFS	NEMO (OCRA025)	H-TESEL
HadGEM3-GC31-HH	Met Office Hadley Centre, UK	HighResMIP	r1i1p1f1	768 × 1,024	MetUM-HadGEM3-GA7.1	NEMO-HadGEM3-GO6.0	JULES-HadGEM3-GL7.1
HadGEM3-GC31-HM	Met Office Hadley Centre, UK	HighResMIP	r1i1p1f1	768 × 1,024	MetUM-HadGEM3-GA7.1	NEMO-HadGEM3-GO6.0	JULES-HadGEM3-GL7.1
HadGEM3-GC31-LL	Met Office Hadley Centre, UK	HighResMIP	r1i1p1f1	144 × 192	MetUM-HadGEM3-GA7.1	NEMO-HadGEM3-GO6.0	JULES-HadGEM3-GL7.1
HadGEM3-GC31-MM	Met Office Hadley Centre, UK	HighResMIP	r1i1p1f1	324 × 432	MetUM-HadGEM3-GA7.1	NEMO-HadGEM3-GO6.0	JULES-HadGEM3-GL7.1

Note: Historical, RCP8.5 experiments are CMIP5 simulations, while HighResMIP are CMIP6 simulations.

of 1995–2014 was selected as the baseline period since it has been commonly used in previous studies (Mudryk *et al.*, 2020; Tokarska *et al.*, 2020).

2.2 | Climate indices

Besides the two mean climate indices of mean temperature (Tas) and daily precipitation (Pr), four extreme climate indices were analysed. These were the annual maxima of daily maximum temperatures (TXx), the annual minima of daily minimum temperatures (TNn), the annual maximum 1-day precipitation (Rx1day) and the maximum consecutive number of dry days (CDD). Details regarding the indices are provided in Table 2. The four extreme indices were defined by the Expert Team on Climate Change Detection and Indices (ETCCDI; Frich *et al.*, 2002; Shi *et al.*, 2017). Model performance and climate projection were determined in terms of these six indices, which represent mean and extreme climate. Three river basins were chosen for analysis (Figure 1), each with a different regional climate. The regional temperature and precipitation over each basin were analysed for all sources.

2.3 | Evaluation method

The CMIP5 and CMIP6 models were evaluated in terms of their ability to reproduce the spatial distributions and interannual variations of the six climate indices over China. Two skill scores were used, the Taylor skill score (TSS; Taylor, 2001) and the interannual variability skill score (IVS; Chen *et al.*, 2011). Model skill was evaluated for the 45-year historical period of 1961–2005.

The Taylor skill score (TSS) was used to evaluate the spatial distribution of the climatology. Using CN0.1 data as the reference data, and the score is defined as

$$TSS = 4(1+R)^2 / \left[\left(\frac{\sigma_{obs}}{\sigma_{cmip}} + \frac{\sigma_{cmip}}{\sigma_{obs}} \right) (1+R_0)^2 \right], \quad (1)$$

where R is the spatial correlation coefficient between the reference data and CMIP model output values, and $R_0 = 1$ is the highest R achievable. σ_{cmip} and σ_{obs} represent the spatial standard deviation of the simulated and observed patterns, respectively. The $TSS \sim 1$ threshold value indicates perfect association between model and observed, whereas $TSS = 0$ expresses contrary model performance. This technique has been used in previous studies such as Xin *et al.* (2020) and Zhu *et al.* (2020).

The interannual variability skill score (IVS) was used to evaluate temporal (interannual) variations in the models, that is, how well the models reproduced the reference temporal standard deviation. Using CN0.1 data as the reference data, and the score is defined as

$$IVS = \left(\frac{STD_0}{STD_m} - \frac{STD_m}{STD_0} \right)^2,$$

where STD_0 and STD_m denote the interannual standard deviation of the reference and the simulations, respectively. IVS is a symmetric statistic that filters out

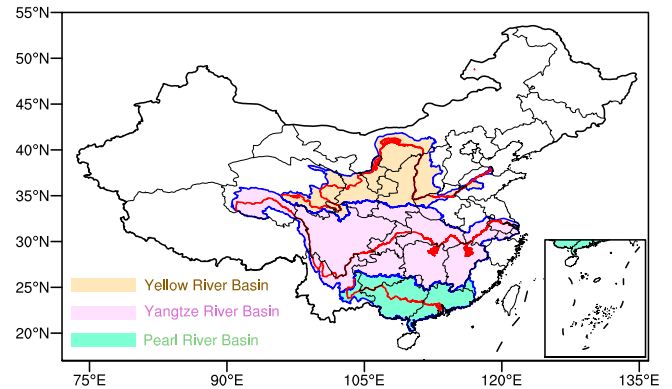


FIGURE 1 The locations of the three major river basins evaluated in this study: Yellow River basin (yellow shading), Yangtze River basin (purple shading), and Pearl River basin (green shading). Red lines indicate the three rivers

TABLE 2 Definition of climate extreme indices analysed in this study

Number	Indices	Descriptive name	Definition	Units
1	TXx	Max Tmax	The annual maxima of daily maximum	°C
2	TNn	Min Tmin	The annual minima of daily minimum	°C
4	Rx1day	Maximum 1-day precipitation	Annual maximum consecutive 1-day precipitation	mm
5	CDD	Consecutive dry days	Maximum number of consecutive dry days (when PR < 1.0 mm)	days

Note: The abbreviations are TX daily maximum temperature, TN daily minimum temperature and PR daily precipitation.

interdecadal signals, and smaller IVS values indicate better performance of the model simulation.

3 | RESULTS

3.1 | Observed historical changes

Figure 2a–c shows the spatial patterns of changes in annual and seasonal mean temperature (Tas) over China for the period of 1961–2018. Tas has significantly increased by more than 1.0°C over most parts of China (Figure 2a), with significantly stronger warming in winter than in summer (Figure 2b,c). Warming over the Yellow River basin was significantly stronger than over the

other two basins. The east part of Yangtze River Basin alone showed no statistically significant warming in summer. Figure 2d–f shows the time series of Tas anomaly over China and three river basins, and despite strong inter-decadal oscillations, the upward trends were statistically significant. Figure 2g–i shows the increases of annual, summer and winter Tas over different regions from 1961 to 2018. Tas over China has increased by 1.7, 2.2 and 1.2°C for the whole year, winter and summer, respectively. Tas over the Yellow River basin has increased by 1.8, 2.6 and 1.3°C for the whole year, winter and summer, respectively. Tas over the Yangtze River basin has increased by 1.1, 1.5 and 0.6°C for the whole year, winter and summer, respectively. Tas over the Pearl River basin has increased by 1.0, 1.3 and 0.7°C for the

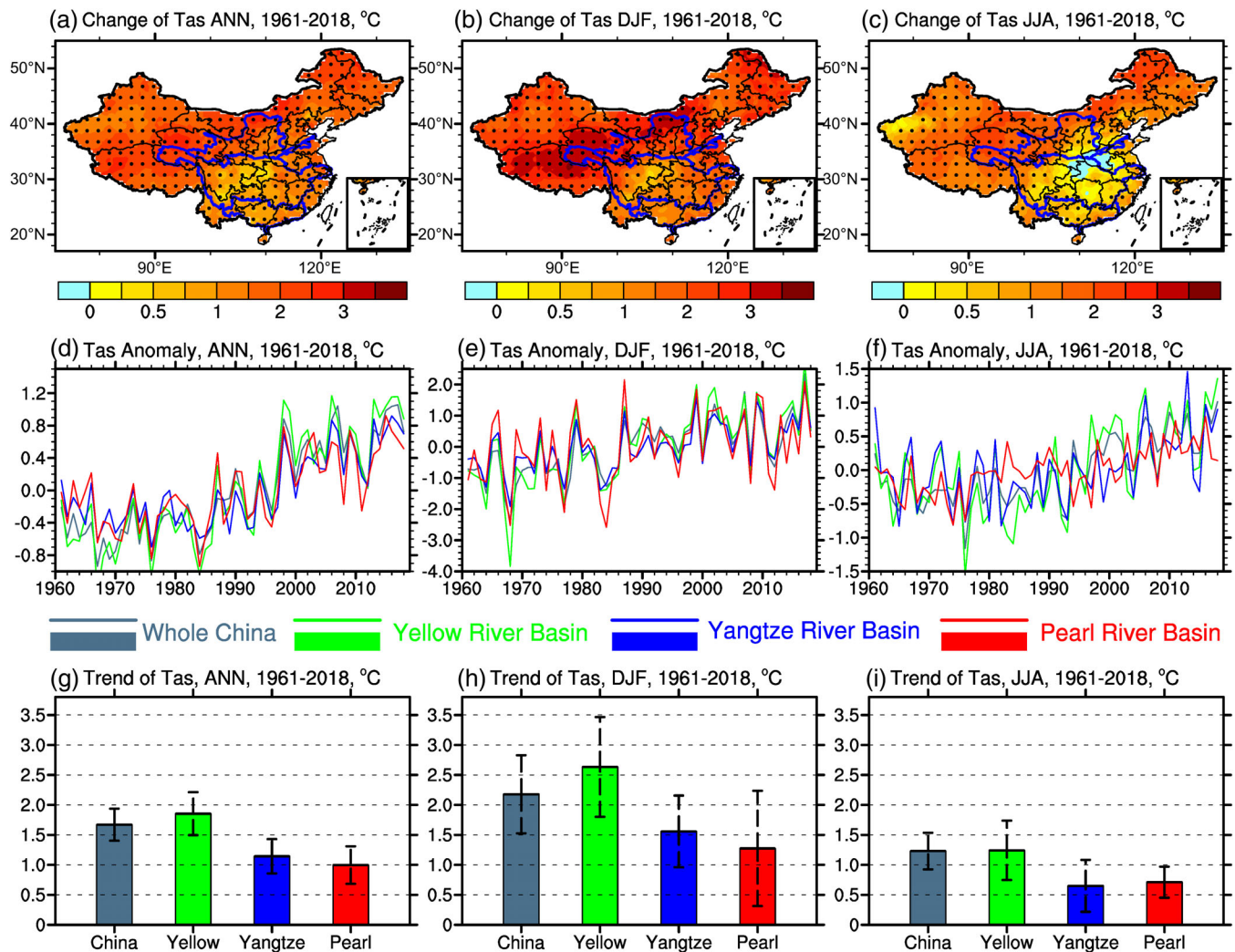


FIGURE 2 The observed changes of annual and seasonal temperature during 1961–2018 over the whole of China (grey), the Yellow River basin (green), the Yangtze River basin (blue), and the Pearl River basin (red). The dotted regions (a–c) significance at 95% confidence level using the 2-tailed Student's *t* test. Error bars (g–i) indicate the 95% confidence interval

whole year, winter and summer, respectively. The warming was the strongest over the Yellow River basin and weakest over the Pearl River basin.

Figure 3a–c shows the spatial patterns of changes in annual and seasonal mean precipitation (Pr) over China for the period of 1961–2018. Pr has significantly increased in the northwestern and southeastern parts of China and significantly decreased in the southwestern and northern parts of China. Pr changes were largest in summer, reflecting the large baseline monsoon precipitation. Figure 3d–f shows the time series anomalous of Pr over China and three river basins. While the upward trend over the Yangtze River Basin was statistically significant, the precipitation trends over the Yellow River and Pearl River basins were not. Unlike mean temperature (Tas) with clear upward trends over all the study regions, precipitation trends were not visibly apparent due to their large inter-decadal variability. The amplitude of inter-decadal oscillations over the Pearl River basin was

particularly large compared to that over the other two basins. Figure 3g–i shows the increases of Pr over different regions from 1961 to 2018. Pr over China has increased by about the same $0.1 \text{ mm}\cdot\text{day}^{-1}$ for the whole year, winter and summer. The changes of Pr over Yellow River and Pearl River basins were not statistically significant. Pr over the Yangtze River basin increased by 0.2, 0.2 and 0.5 mm for the whole year, winter and summer, respectively.

Figure 4 shows the observed changes of extreme temperature (TXx, TNn) and precipitation (Rx1day, CDD) over China for the period of 1961–2018. Figure 4a–c shows that the annual maxima of daily maximum temperature (TXx) has significantly increased by 1.2°C over most parts of China. TXx over the Yellow, Yangtze and Pearl River basins has increased by 1.5, 1.2 and 1.0°C , respectively. Like Tas, the increase of TXx was largest over the Yellow River basin. The increase of TXx over the Yangtze River basin was about the same as the increase

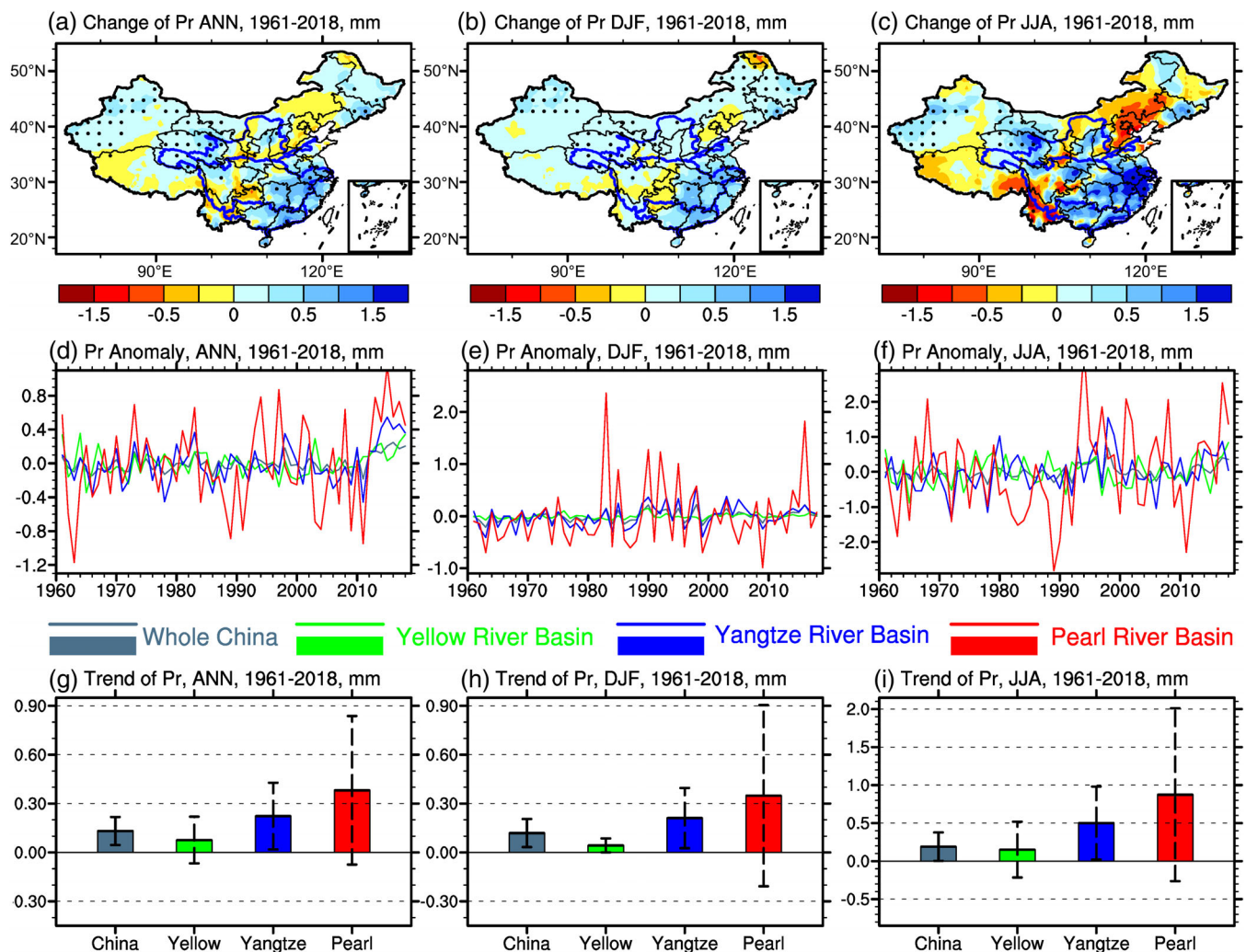


FIGURE 3 Similar to Figure 2, but for precipitation

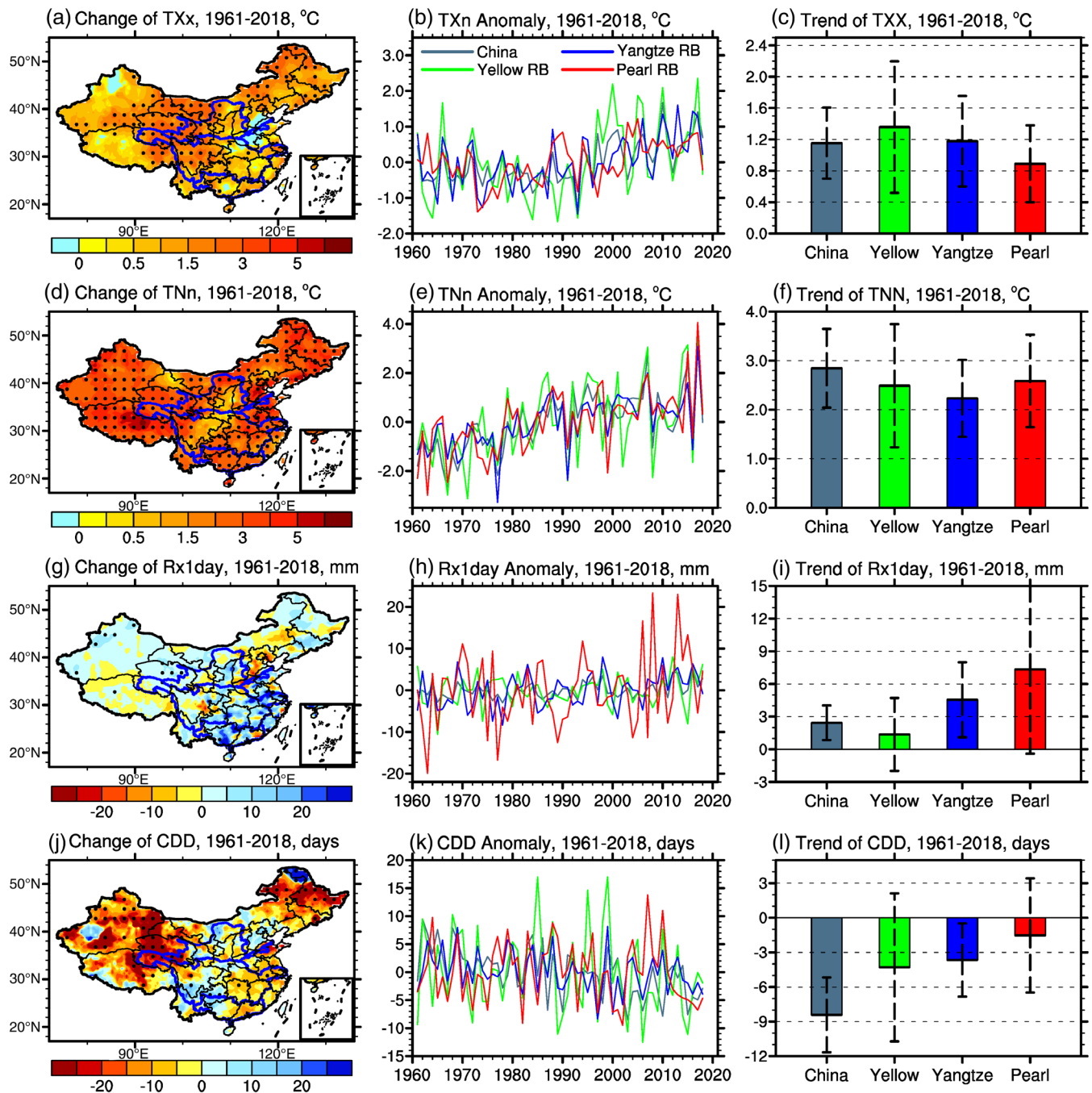


FIGURE 4 The observed spatial and temporal variations of extreme indices. (a–c) TXx, (d–f) TNn, (g–i) Rx1day, (j–l) CDD during 1961–2018. The dotted regions (a, d, g, j) significance at 95% confidence level using the 2-tailed Student's *t* test. Error bars (c, f, i, l) indicate the 95% confidence interval

over the whole of China, while that over the Pearl River basin was smaller. Stronger changes were seen in the annual minima of daily minimum temperatures (TNn), as shown in Figure 4d–f. The increase of TNn over China reached 2.8°C, while increases over Yellow, Yangtze and Pearl River basins reached 2.5, 2.2 and 2.6°C, respectively. While the increases of whole-year Tas and TXx

over the Pearl River basin were the smallest of the three basins, the increase of TNn was the largest.

Figure 4g–i shows that the annual maximum 1-day precipitation (Rx1day) over China has significantly increased by 2.0 mm. However, the local trend of Rx1day was spatially uneven; Rx1day has increased in the south-east coastal area, decreased in north, but showed no

obvious trend in the northwest. Almost none of these local values were statistically significant. Rx1day over the Yellow River basin showed no statistically significant increase. Rx1day over the Yangtze and Pearl River basins has increased by 7.0 and 5.0 mm, respectively. Figure 4j–l shows that the maximum consecutive number of dry days (CDD) over China has decreased by 8 days (during the past 54 years, or $1.5 \text{ days-decade}^{-1}$). Large decreases were seen over most parts of northwest and northeast China. CDD over the Yellow River basin showed no statistically significant decrease, although its 4 days reduction was large in value. CDD over the Yangtze and Pearl River basins has reduced by 4 and 1 day, respectively.

Overall, there has been significant warming over most of China in the past six decades, with warming in winter stronger than that in summer (Figure 2). The warming over the Yellow River basin was significantly stronger than that of over the Yangtze River and Pearl River basins. Both TXx and TNn has increased significantly, and the increase of TNn was much larger than that of TXx. Unlike temperature, the spatial pattern of precipitation change was more complex, with some regions wetting and some drying (Figure 3). The uncertainty in precipitation change was large, with only a few regions showing statistically significant changes, mainly wetting. Precipitation changes over the three river basins were the same in sign. Pr and Rx1day have increased, while CDD has decreased. The largest increases of Pr and Rx1day were seen over the Pearl River basin, but these values were not statistically significant because the region also had the largest variability in precipitation.

3.2 | Verification of individual models

The Taylor skill score (TSS; Taylor, 2001) and inter-annual variability skill score (IVS; Chen *et al.*, 2011) scores were used to evaluate the simulation of temperature indices (Tas, TNn, TXx) and precipitation indices (Pr, Rx1day, CDD) over China for the period of 1961–2005. The spatial characteristics of China's temperature and precipitation were generally well-reproduced by most of the models, in terms of both climate mean and extreme events. The exceptions were TXx and CDD in certain CMIP5 models. As a group in general, whether CMIP5 or CMIP6, temperature was simulated better than precipitation over China. The CMIP6 models as a group showed clear improvements over CMIP5 models, particularly for the precipitation indices. The caveat is that the performances of individual models differ widely within groups.

Figure 5 shows the TSS of the six climate indices, used to quantify the models' ability to simulate the spatial

patterns of annual climatological fields. The higher the value of TSS, the better the simulation. The threshold value of 0.6 was used to classify if the pattern was well-simulated.

Figure 5a shows that the spatial distribution of annual mean temperature over China (Tas) was extremely well-simulated by all models, with its TSS close to 1 for all of the CMIP5 and CMIP6 models. TSS of Tas exceeded 0.95 for two CMIP5 models and five CMIP6 models. These best performers were the CMIP5 models CCSM4 and EC-EARTH, the CMIP6 model EC-Earth3P, and the four CMIP6 HadGEM3-GC31 models. We now discuss TNn before TXx. The TSS of TNn were similarly high, exceeding 0.8 for all of the eight CMIP5 and eight CMIP6 models (Figure 5c). The best performers for simulating TNn were MRI-CGCM3, EC-EARTH, EC-Earth3P and HadGEM3-GC31-HH. In contrast with Tas and TNn, models show considerable bias in TXx. The TSS of TXx was lower than 0.6 for every model (Figure 5b). It fell even below 0.4 for three CMIP5 models and one CMIP6 model. The CMIP6 model in question was HadGEM3-GC31-LL, the lowest resolution version of HadGEM3-GC31; the other three versions of HadGEM3-GC31 with higher resolutions performed slightly better. The relatively better performers were the three EC-EARTH models of EC-EARTH (CMIP5), EC-Earth3P and EC-Earth3P-HR (CMIP6), as well as CMIP6 model CNRM-CM6-1-HR.

Figure 5d shows that the spatial distribution of annual mean precipitation over China (Pr) was still well-simulated, with its TSS exceeding 0.6 for all models. However, the precipitation was not as well-simulated as temperature, and the TSS of Pr did not exceed 0.9 for any model. The best performers for simulating Pr were the CMIP5 models CanESM2 and EC-EARTH, and the CMIP6 models of EC-Earth3P and EC-Earth3P-HR. Figure 5e shows that Rx1day was also well-simulated, with the exception of two CMIP5 models. The TSS of Rx1day exceeded 0.6 for all models except the CMIP5 models BNU-ESM and FGOALS-g2. The CMIP6 models as a group performed better than the CMIP5 models; four of the eight CMIP5 models had TSS more than 0.1 lower than the minimum TSS of the CMIP6 models (~ 0.75). For all CMIP6 models, the best performers for simulating Rx1day were CNRM-CM6-1, CNRM-CM6-1-HR, HadGEM3-GC31-LL and HadGEM3-GC31-MM. TSS was lower for the two higher resolution HadGEM3-GC31-HH and HadGEM3-GC31-HM compared to the two lower resolution version. Figure 5f shows that CDD was only well-simulated in three of the CMIP5 models—CanESM2, EC-EARTH and MRI-CGCM3. The TSS of CDD fell below 0.6 for all other CMIP5 models. In contrast, the TSS scores for all CMIP6 models exceeded 0.6.

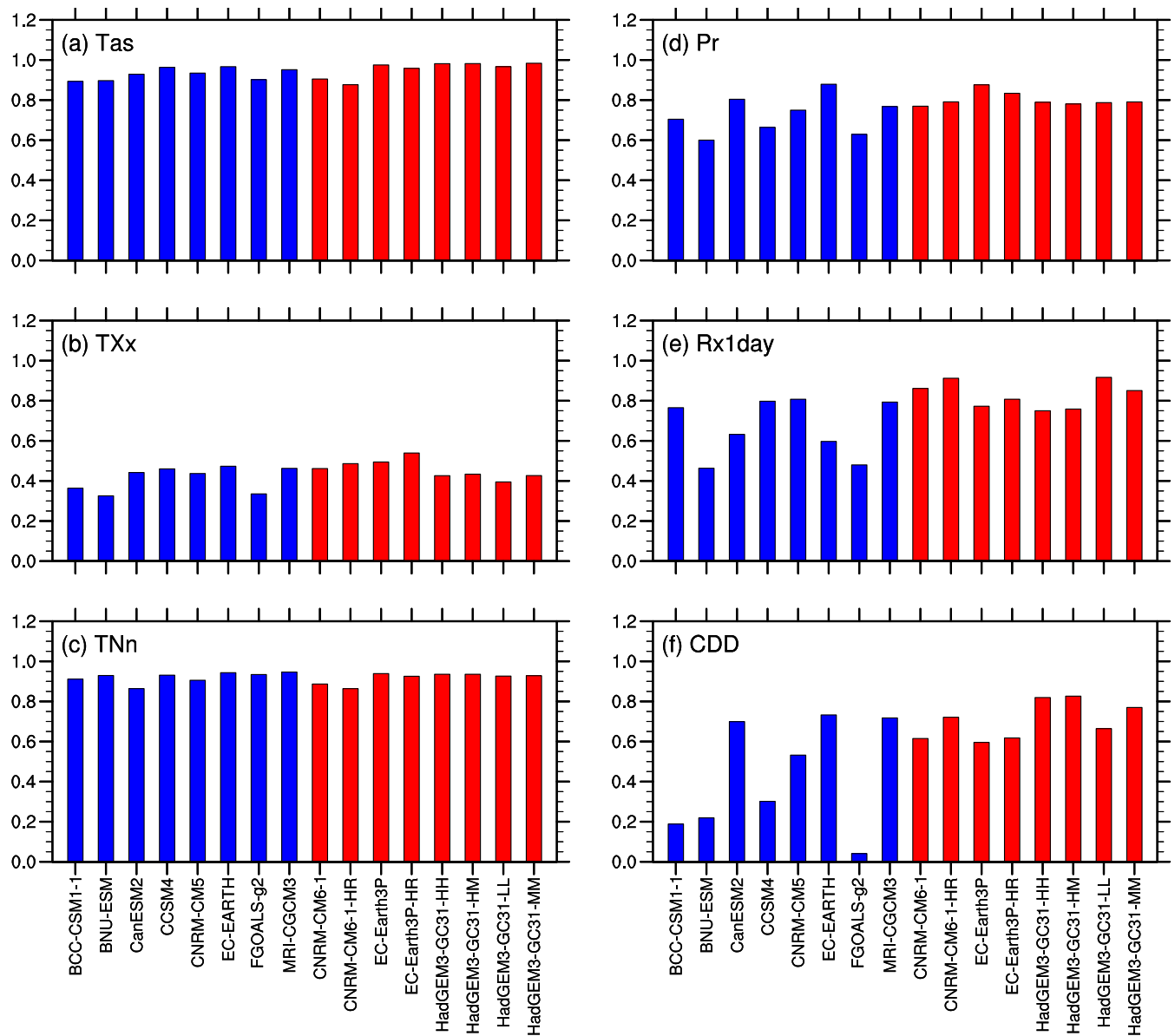


FIGURE 5 Skill scores in terms of TSS showing the performance of models (CMIP6 in red, CMIP5 in blue) in simulating annual climatological fields over China for Tas (a), TNn (b), TXx (c), Pr (d), Rx1day (e) and CDD (f)

The CMIP6 models as a group clearly performed better than the CMIP5 models. The other five of the CMIP5 models had TSS lower than the minimum TSS of the CMIP6 models. The best performing CMIP6 models for simulating CDD were the HH, HM and MM versions of HadGEM3-GC31.

Figure 6 shows the IVS of the six climate indices, used to quantify models' ability to simulate interannual variation over China. The lower the value of the IVS, the better the simulation. Different thresholds were used for different climate indices to classify if interannual variation was well-simulated. Figure 6a shows that the performance for mean temperature over China (Tas) varied greatly between

models. Interannual variation was well-simulated by half of the models with IVS less than 0.1. These were the three CMIP5 models of BCC-CSM1-1, EC-EARTH and FGOALS-g2, and five CMIP6 models which were EC-EARTH3P-HR and the four versions of HadGEM3-GC31. Simulation was poor for three models with IVS exceeding 0.3, the CMIP5 model BNU-ESM, and two CMIP6 models CNRM-CM6-1 and EC-Earth3P. Like for the discussion of TSS, TNn will be discussed here before TXx. Figure 6c shows IVS of TNn, also with very different performance between models. Interestingly, the CMIP5 models as a group performed better than the CMIP6 models. The best performers were CanESM2, CCSM4, CNRM-CM4 and

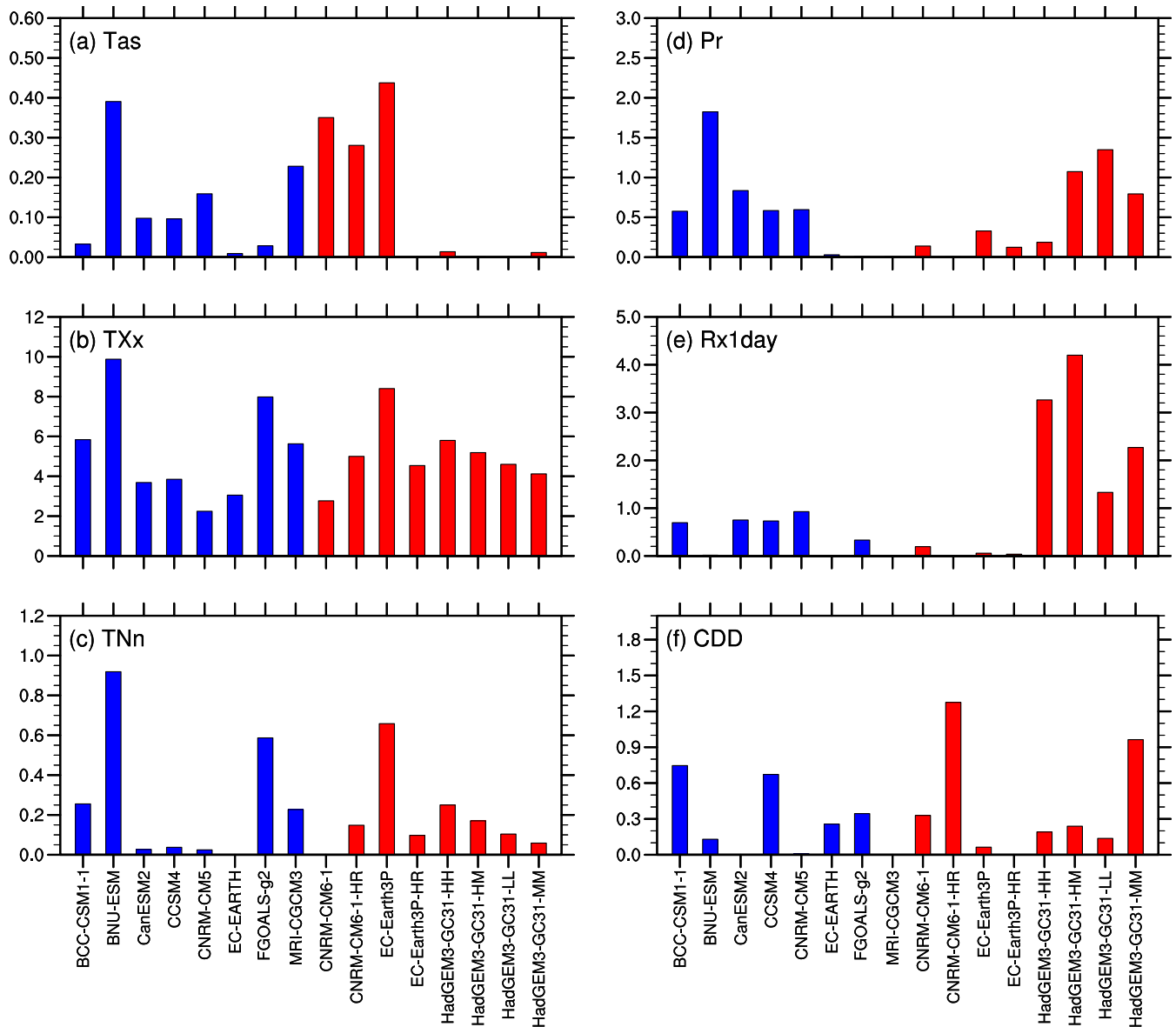


FIGURE 6 Skill scores in terms of IVS showing the performance of models (CMIP6 in red, CMIP5 in blue) in simulating temporal variation over China for Tas (a), TNn (b), TXx (c), Pr (d), Rx1day (e) and CDD (f)

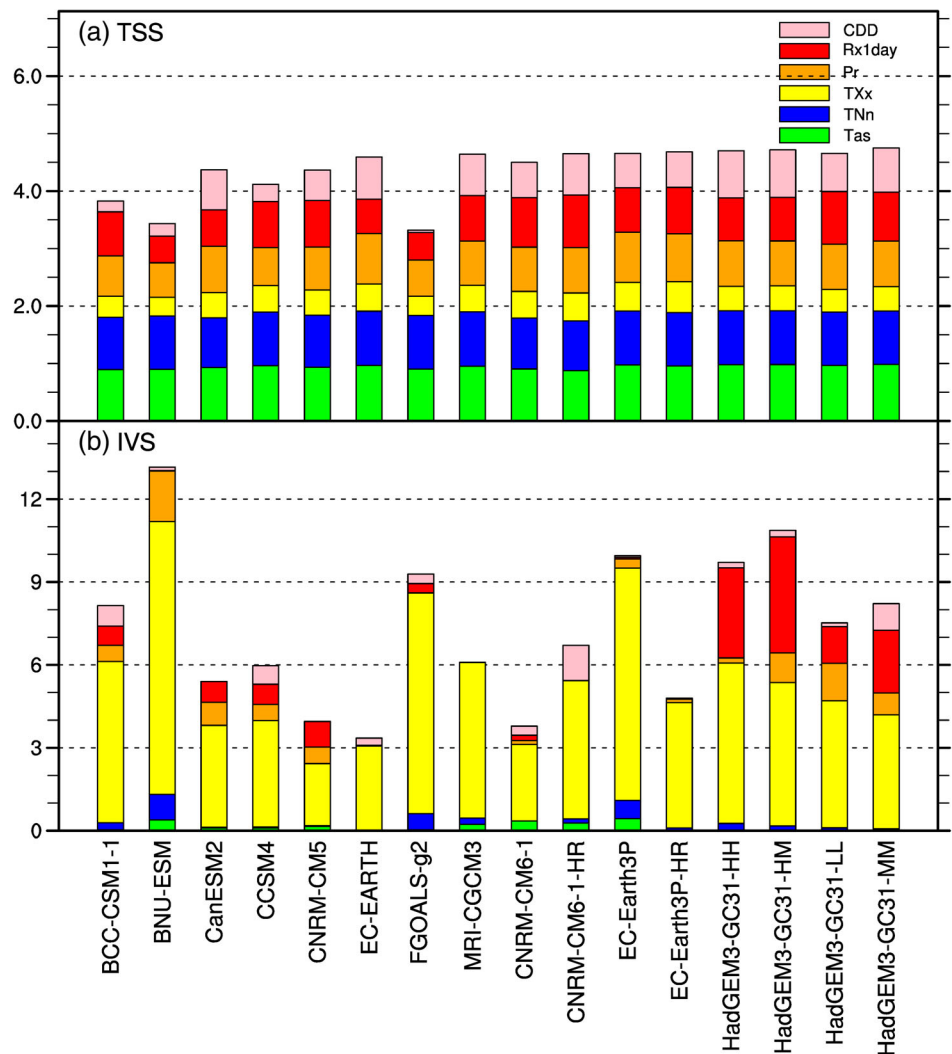
EC-EARTH of all CMIP5 models. The worst performer was also a CMIP5 model, BNU-ESM with IVS of 0.9. The relatively better performers were CMIP5 models CNRM-CM5 and EC-EARTH, and CMIP6 model CNRM-CM6-1. Figure 6b shows the IVS of TXx, which exceeded 4.0 for most of the models, indicating that interannual variation of TXx was poorly simulated. The IVS value of BNU-ESM was the largest at about 10. The overall poor performance simulating interannual variation was consistent with the poor performance simulating spatial distribution, previously concluded from the TSS results. Figure 6d–f shows the IVS of precipitation indices. Similar to the temperature indices, the performance varied greatly between models. Some models performed well for one precipitation index,

but poorly for another. This indicated large uncertainties exist when drawing conclusions about precipitation from individual models.

To intuitively assess the overall performance of CMIP5 and CMIP6 models over China, the sum of TSS and IVS across indices are shown in Figure 7a,b, respectively. Since there are six climate indices, a total TSS closer to 6.0 indicates a better simulation. A smaller total IVS indicates a better simulation.

From Figure 7a, total TSS exceeded 4.0 for four CMIP5 models and all eight CMIP6 models. The total TSS for the CMIP6 models was consistently high, with scores between 4.5 and 5.0. In contrast, the total IVS varied widely between individual CMIP5 models. Total TSS

FIGURE 7 Sum scores in terms of TSS (a) and IVS (b) showing the performance of CMIP5 and CMIP6 models in simulating climatology and interannual variation over China for Tas (green), TNn (blue), TXx (yellow), Pr (orange), Rx1day (red) and CDD (pink)



fell below 4.0 for BCC-CSM1-1, BNU-ESM and FGOALS-g2, indicating poor performance. From Figure 7b, total IVS varied widely between individual CMIP5 and CMIP6 models. The best performers (lowest total IVS) were CMIP5 models CNRM-CM5 and EC-EARTH, and CMIP6 models CNRM-CM6-1 and EC-Earth3P-HR. The combined results of TSS and IVS indicated that in comparison with observed climatology, the spatial distributions of temperature and precipitation were well-simulated, but interannual variations less well so. In view of this variable performance, the multi-model ensemble means (MME) of CMIP5 and CMIP6 models will be used for climate projections in the sections below.

3.3 | Verification of multi-model ensemble means

The results presented in this section are based on the CMIP5 and CMIP6 multi-model ensemble means (MMEs). Figure 8 shows the climatological pattern and

change of the temperature climate indices (Tas, TXx, TNn) over China for the period of 1961–2005. From Figure 8a, observed mean temperature (Tas) was higher over southeast China, lower over northwest and northeast China, and lowest over the Qinghai-Tibet Plateau in southwest China. The maximum and minimum mean temperatures were about 22 and -10°C , respectively. From Figure 8b,c, this spatial pattern was well-reproduced by both CMIP5 and CMIP6 MMEs. The minimum Tas was lower in the two MMEs compared to observation, due to negative bias over the Qinghai-Tibet Plateau. Figure 8d shows the change of Tas from 1961 to 2005. Both CMIP5 and CMIP6 MMEs underestimated the warming of Tas over China. For the river basins, both MMEs underestimated warming over the Yellow River basin and overestimated warming over the Yangtze River basin. The CMIP5 MME overestimated the warming over the Pearl River basin, while the CMIP6 MME underestimated it.

From Figure 8e, the spatial pattern of the annual maxima of daily maximum temperatures (TXx) looked

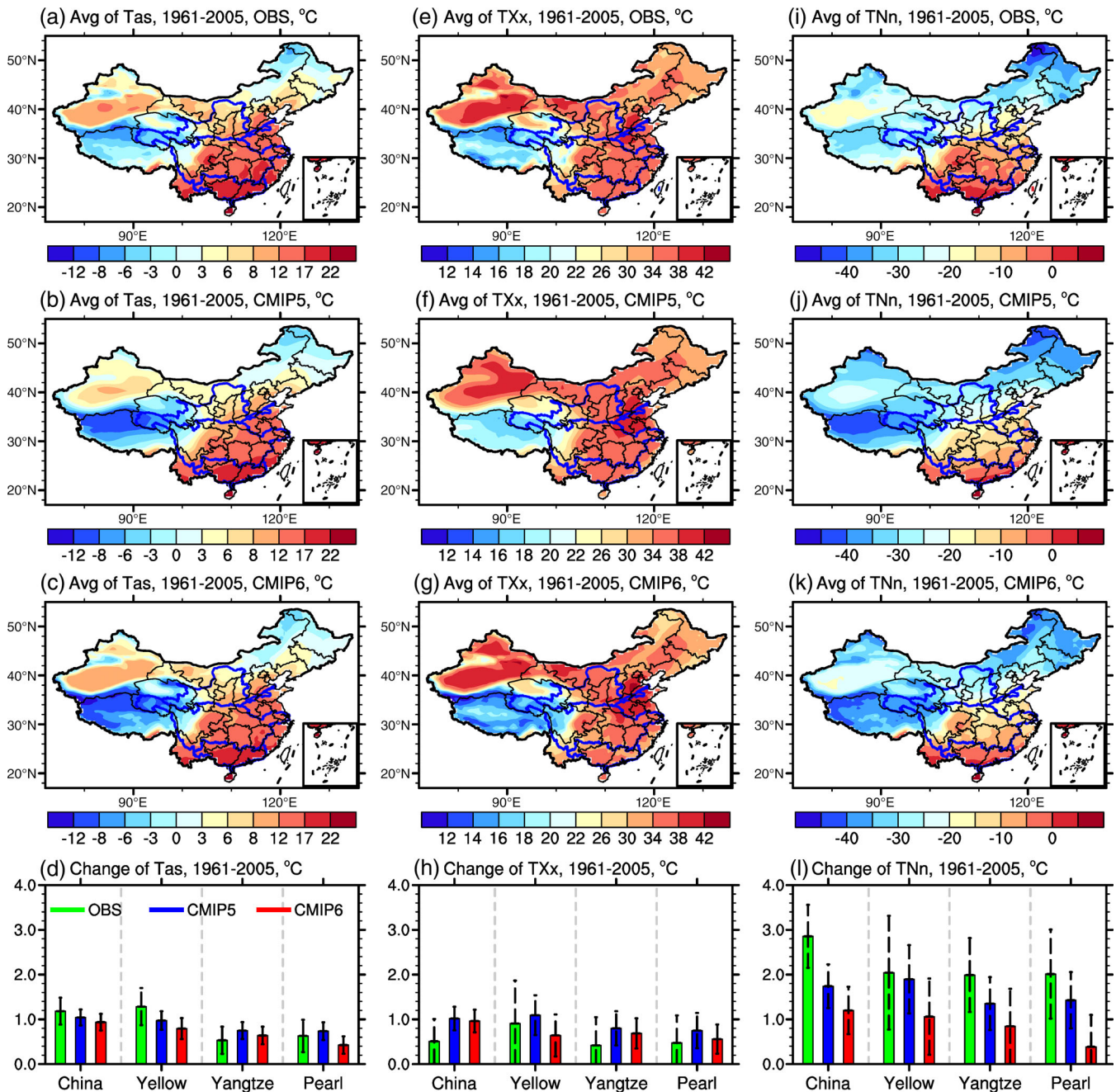


FIGURE 8 The climatological pattern and change of Tas, TXx and TNn during 1961–2005 over China, calculated from the CMIP5 MME and the CMIP6 MME. Error bars indicate significance at 95% confidence level using the 2-tailed Student's *t* test

quite similar to the spatial pattern of Tas. From Figure 8f, g, the spatial pattern of TXx was well-reproduced by both CMIP5 and CMIP6 MMEs. Like Tas, TXx was less well-simulated over the Qinghai-Tibetan Plateau, with warming overestimated by the CMIP5 MME and underestimated by the CMIP6 MME. Figure 8h shows the change of TXx from 1961 to 2005. Both CMIP5 and CMIP6 MMEs overestimated the warming over China. For the river basins, both MMEs overestimated the

warming over the Yangtze River and the Pearl River basins. The CMIP5 MME overestimated the warming over the Yellow River basin, while the CMIP6 MME underestimated it.

Figure 8i–k shows that for the annual minima of daily minimum temperatures (TNn), both CMIP MMEs agree well with observation in terms of spatial pattern, but were biased low over the cool Qinghai-Tibet Plateau and warm southern China. Figure 8l shows the change of

TNn from 1961 to 2005. Observed TNn has increased over China and all three river basins. This increase was clearly larger than the increase of Tas and TXx. Both MMEs underestimated this increase, and the CMIP6 MME performed worse.

Figure 9 shows the climatological pattern and change of the precipitation climate indices (Pr, Rx1day, CDD) over China for the period of 1961–2005. From Figure 9a, mean daily precipitation (Pr) over China for the period of 1961–2005 was lower over northwest China and higher

over southeast China. From Figure 9b,c, this spatial pattern was well-reproduced by both CMIP5 and CMIP6 MMEs. Over dry northwest China, the CMIP5 MME had a positive bias (wetter), while the CMIP6 MME matched observation better. Figure 9d shows the change of Pr from 1961 to 2005. The results from both MMEs were clearly different from observation. This was especially so over the Yellow River basin, where the observed change was negative (but not statistically significant). Both MMEs produced positive change

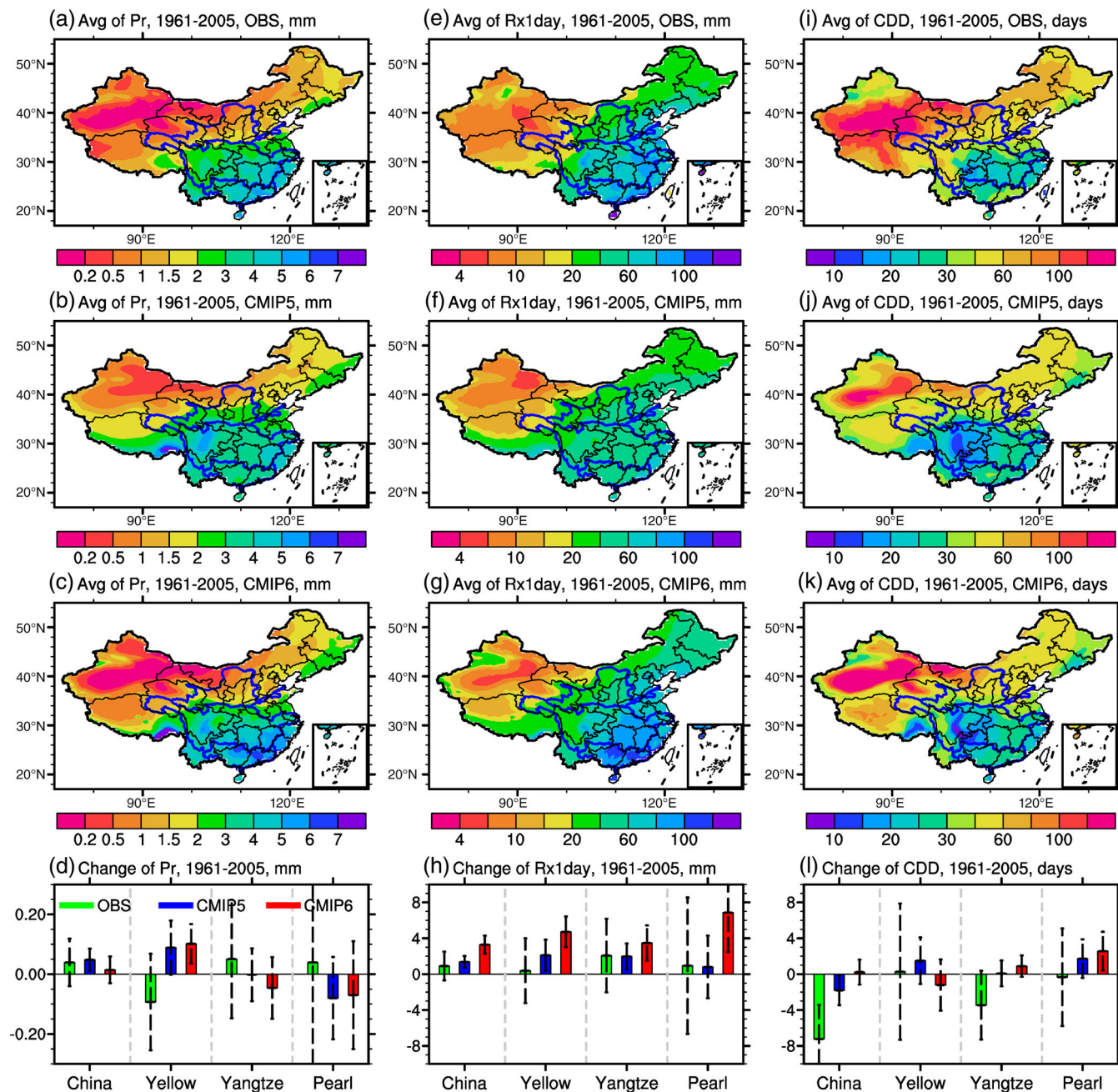


FIGURE 9 The climatology distribution and trend of Pr, Rx1day and CDD during 1961–2005 over China, calculated from the CMIP5 MME and the CMIP6 MME. Error bars indicate significance at 95% confidence level using the 2-tailed Student's *t* test

instead. Over the Pearl River basin, the observed change was positive, but both MMEs produced negative changes. In this case, none of the results were statistically significant since uncertainty (confidence interval) was the largest over the Pearl River basin.

From Figure 9e–g, the spatial pattern of the annual maximum 1-day precipitation (Rx1day) was well-reproduced by both MMEs, with no outstanding biases. Figure 9h shows the change of Rx1day from 1961 to 2005. The results from both MMEs were of the same sign as the observed change, but had positive biases (wetter). The bias was especially large for the CMIP6 MME over the Pearl River basin.

From Figure 9e,f, spatial pattern of the maximum consecutive number of dry days (CDD) had notable biases in both MMEs. This occurred mainly over the high values (drier) over northwest China. The coverage of these high values was smaller in the MMEs compared to observation. Similar to the average precipitation, the model had significant deviation of CDD evolution trend in different regions of China between the simulation results and the observed values. From Figure 9g, the change of CDD from 1961 to 2005 was clearly biased in the MMEs.

In summary, the CMIP5 and CMIP6 MMEs reproduced the spatiotemporal characteristics of temperature and precipitation over China, both in terms of mean and extremes. The spatial patterns of the climate indices were in good agreement with observation. From visual inspection, the CMIP6 spatial patterns appear improved from CMIP5. However, the time change of the climate indices model showed large biases for TNn and the precipitation indices. Changes in the precipitation indices were even of opposite sign from observation when the analysis was performed for individual river basins in China. Current earth system models are relatively reliable for temperature analysis, but uncertainty is large for precipitation analysis. Precipitation changes over individual river basins should not be used.

3.4 | Near-term climate projections

Climate projections of temperature and precipitation over China were calculated from the CMIP5 and CMIP6 MMEs. The RCP8.5 scenario was used for the CMIP5 models, while the CMIP6 models were taken from the HighResMIP experiment. The HighResMIP experiment was compared against RCP8.5 because its emissions were based on RCP8.5; hence, the CMIP5 RCP8.5 simulations and the CMIP6 HighResMIP simulations were most comparable.

Figure 10 shows the projected changes of temperature indices (Tas, TXx and TNn) for the period of 2015–2050. From Figure 10a–c, Tas will increase significantly over all of China. From the CMIP5 MME, the increase over cool northwest China will be larger than over warm southeast China. In contrast, the CMIP6 MME showed uniform warming throughout China. From Figure 10c, Tas over China will increase by 1.4 and 2.0°C, from the CMIP5 and CMIP6 MME, respectively. From the CMIP5 MME, Tas over the Yellow, Yangtze and Pearl River basins will increase by 1.5, 1.4 and 1.0°C, respectively. From the CMIP6 MME, the values will be 2.2, 2.0 and 1.7°C, respectively. The projected warming was clearly stronger from the CMIP6 MME compared to the CMIP5 MME.

From Figure 10d–f, TXx will also increase significantly over China. From the CMIP5 MME, TXx will increase by more than 1°C over most of China. The CMIP6 MME predicts a stronger increase of more than 2°C over most of China. From Figure 10f, TXx over China will increase by 1.5 and 2.2°C, from the CMIP5 and CMIP6 MME, respectively. From the CMIP5 MME, TXx over the Yellow, Yangtze and Pearl River basins will increase by 1.4, 1.3 and 1.0°C, respectively. From the CMIP6 MME, the values will be 2.1, 2.3 and 2.0°C, respectively.

From Figure 10g–i, the spatial patterns of TNn change were clearly different between CMIP5 and CMIP6 MMEs. The CMIP5 MME showed significant increases over northwest and northeast China. Increases over central and south China were not statistically significant. The CMIP6 MME show significant increases over most of China. Increases over some regions exceeded 5°C. From Figure 10i, the TNn over China will increase by 1.0 and 2.2°C, from the CMIP5 and CMIP6 MME, respectively. From the CMIP5 MME, TNn over the Yellow, Yangtze and the Pearl River basins will increase by 0.4, 0.6 and 0.5°C, respectively. From the CMIP6 MME, the values will be 2.6, 2.0 and 1.6°C, respectively.

Figure 11 shows the projected changes of precipitation indices (Pr, Rx1day, CDD) for the period of 2015–2050. From Figure 11a–c, the spatial patterns of Pr change were similar in the two MMEs, showing increases (wetting) over most of China. Over south China, the CMIP6 MME predicted a larger increase than the CMIP5 MME. From Figure 11c, Pr over China will increase by 0.15 mm from the CMIP5 MME. From the CMIP5 MME, Pr over the Yellow, Yangtze and Pearl River basins will increase by 0.16, 0.2 and 0.34 mm, respectively. The values from the CMIP6 MME were almost the same as the CMIP5 results, with only the projected increase over the Pearl River basin being much

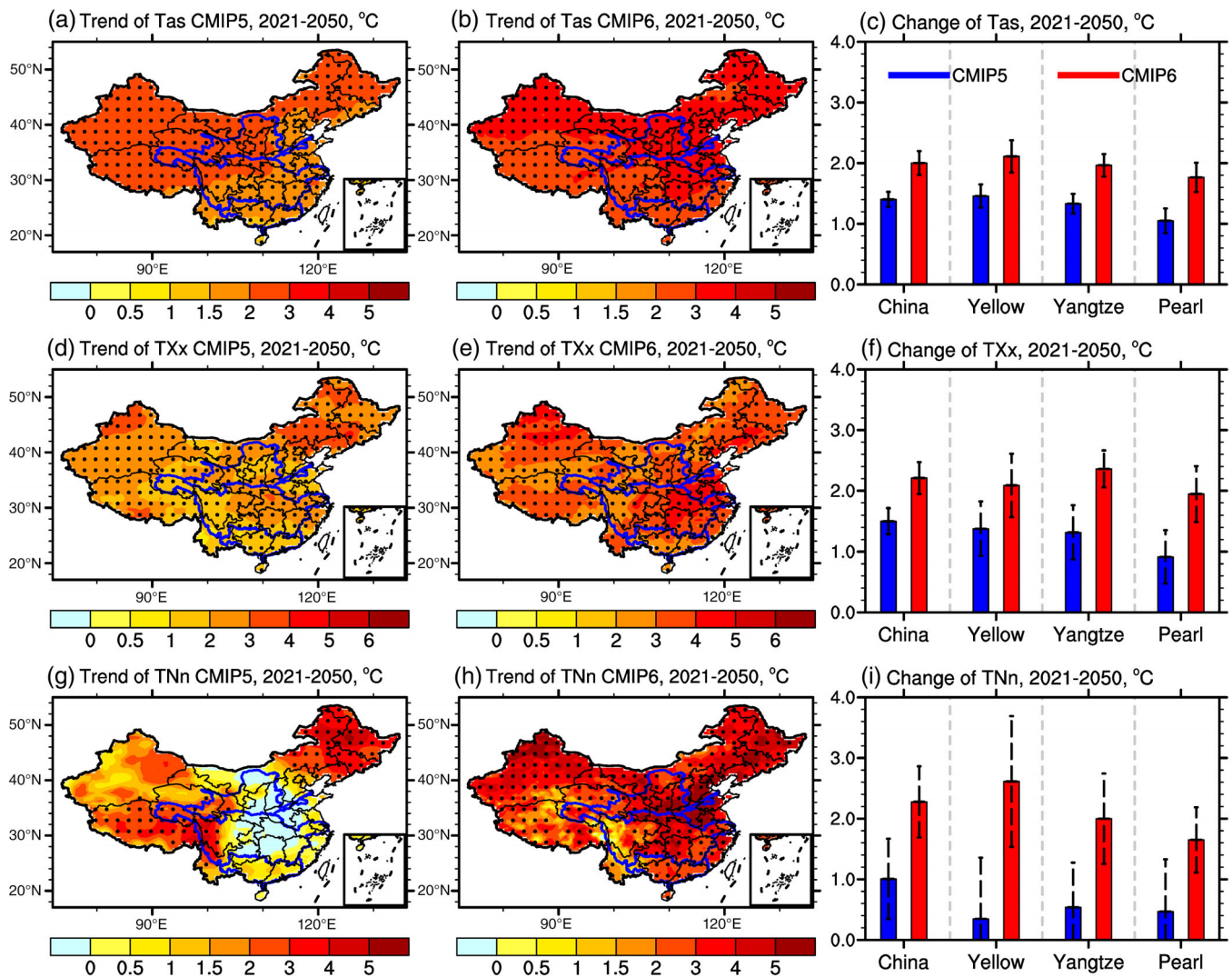


FIGURE 10 The projected changes of Tas, TNn and TXx during 2015–2050, calculated from the CMIP5 MME and the CMIP6 MME, for the whole of China, the Yellow River basin, the Yangtze River basin and the Pearl River basin. Error bars indicate the 95% confidence interval

larger at 0.66 mm, reflecting the differences over south China.

From Figure 11d–f, the spatial patterns of Rx1day change were also similar in the two MMEs, except over the Pearl River basin in south China. From Figure 11f, Rx1day over China will increase by 4 and 5 mm, from the CMIP5 and CMIP6 MME, respectively. From the CMIP5 MME, Rx1day over the Yellow, Yangtze and Pearl River basins will increase by 4, 6 and 10 mm, respectively. From the CMIP6 MME, the values will be 5, 7 and 17 mm, respectively.

From Figure 11g–i, the CMIP5 and CMIP6 MMEs disagree over the sign change of CDD over south China. The CMIP5 MME predicted a decrease (wetter) while the CMIP6 MME predicted an increase (drier). The CMIP6 MME also predicted a much stronger decrease of CDD (wetter) over northwest China. From

Figure 11i, CDD over China will decrease by 3.0 days from both MMEs. From the CMIP5 MME, CDD over the Yellow, Yangtze and Pearl River basins will decrease by 2.0, 0.5 and 2.0 days, respectively. From the CMIP6 MME, CCD will decrease over the Yellow River basin by 4.0 days, but increase over the Yangtze and Pearl River basins by 1.0 and 3.0 days, respectively. The sign difference in changes over the Yangtze and Pearl River basins reflected the disagreement between the two MMEs over south China.

Both CMIP5 and CMIP6 MMEs predicted significant increases in mean temperature (Tas) and extreme temperatures (TXx, TNn) over most of China, with CMIP6 predicting larger increases. The MMEs also predicted increases in precipitation (Pr) and extreme precipitation (Rx1day) over most of China, especially over the Pearl River basin. Again, CMIP6 predicted larger increases.

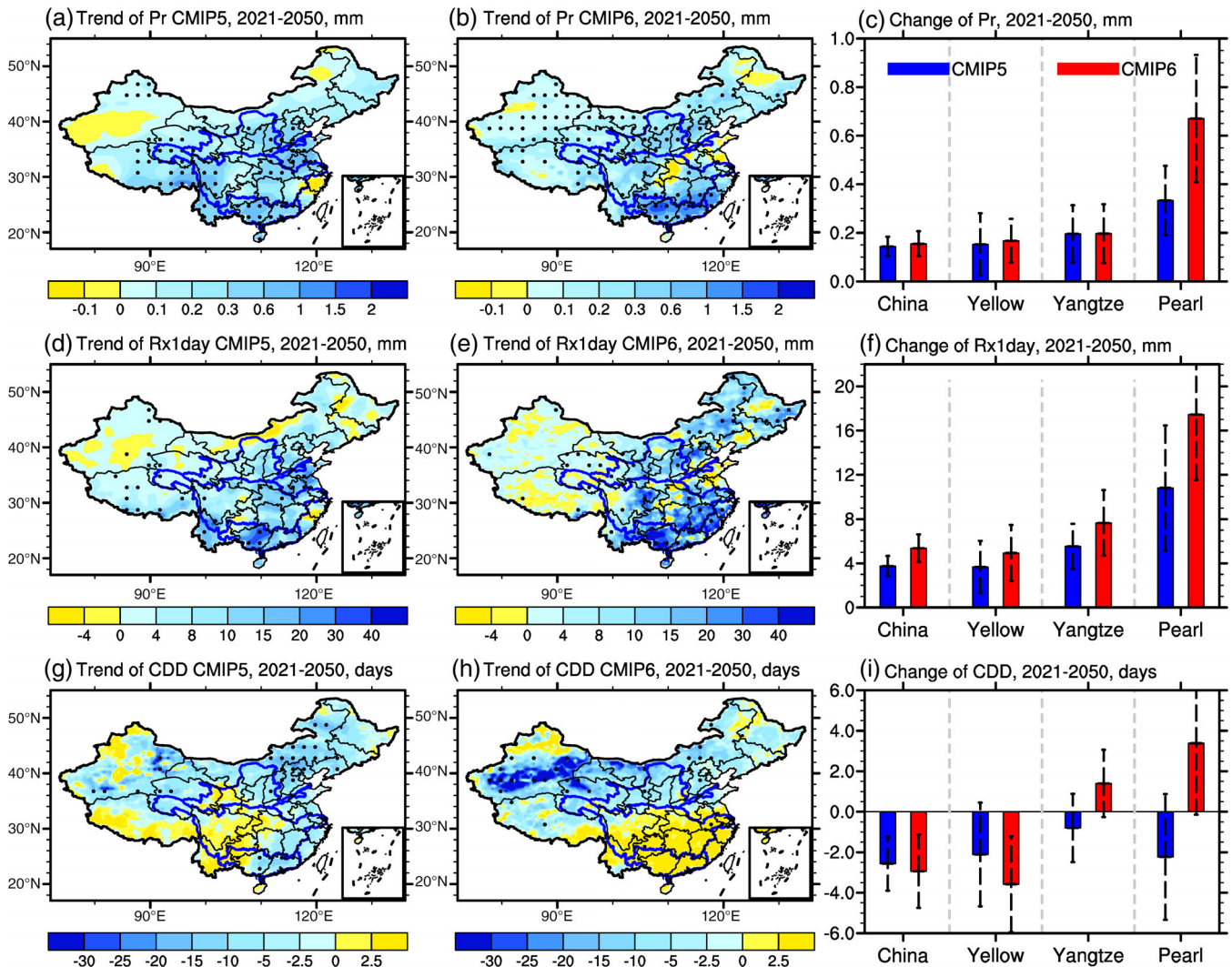


FIGURE 11 Similar to Figure 10, but for Pr, Rx1day and CDD

The local changes in precipitation indices were mostly not statistically significant, but regional statistics were mostly significant except for changes of CDD over individual river basins. Although the two MMEs were in agreement on the sign change of the climate indices, the many of the predicted quantitative values were statistically different between CMIP5 and CMIP6.

4 | CONCLUSION

Historical changes of temperature and precipitation over the Yellow River, Yangtze River and Pearl River basins were evaluated using the high-resolution observation-based dataset CN05.1, eight models from Historical and RCP8.5 experiments in CMIP5, eight models from the HighResMIP experiment in CMIP6 and the CMIP5/6 multi-model ensemble means (MMEs). CN05.1 was used

to assess the performance of the CMIP5/6 simulations. Climate projections up to the year 2050 were then evaluated using the CMIP5 and CMIP6 MMEs.

From the observation-based CN05.1 dataset, most part of China has warmed significantly over the period of 1961–2018, with more severe warming in winter. Temperature over the Yellow River basin has increased by about 1.8°C, greater than the other two basins. Precipitation has increased significantly over the northwestern and southeastern regions of China, but decreased significantly over the southwestern and northern regions of China. Precipitation over the Pearl River basin has increased by about 0.4, 0.35 and 0.8 mm-day⁻¹ for the whole-year, in winter and in summer, respectively, greater than the other two basins. The extreme high and low temperatures have increase significantly which are stronger than the mean temperature over China and the three main river basins. The Rx1day has increased

slightly with the most significant upward trend that has happened over Pearl River basin, and the CDD has decreased. The uncertainty in the change of precipitation was greater than that of temperature.

Most of the CMIP5 and CMIP6 models reproduced the changes of temperature indices better than changes of precipitation indices. The use of MMEs improved the estimations of both temperature and precipitation. The CMIP6 models performed better than the CMIP5 models, especially for temperature changes over the Yangtze River and the Pearl River basins, as well as precipitation changes over the Yellow River and the Pearl River basins. However, this may be due to improvements of the CMIP6 models, the higher resolution of the HighResMIP selection of CMIP6 models, or simply the selection of individual models in the CMIP6 set. At this point we do not know which is outside the scope of this study without analysing the detailed performance of individual models.

Both CMIP5 and CMIP6 MMEs projected warming over the whole of China and the three river basins in the next few decades, with stronger warming projected by the CMIP6 MME, which predict about 2.0°C warming over the whole China and the three river basins during 2021–2050. Both CMIP5 and CMIP6 MMEs projected wetting over the whole of China, but disagree on the spatial pattern of change. The largest disagreement occurred over the Pearl River basin. The CMIP5 MME projected significant wetting during 2015–2050, but the CMIP6 MME projected (nonsignificant) drying during 2015–2050.

When assessing the socio-economic impacts of climate change for China, it is sensible to make targeted climate projections for regions of high population density and economy activity, rather than make combined projections over socio-economically and climatically diverse regions. Much of human activity is concentrated at river basins, yet in the past it has been difficult to resolve the complex boundaries of these basins in coarse resolution global climate models. New high-resolution CMIP6 experiments and the observation-based CN05.1 dataset have now enabled such basin-based evaluations, as was demonstrated in this study. However, there is obvious uncertainty in the projections for the precipitation over the three river basins. Uncertainty in future emissions, internal variability of the climate system and model response are three main sources of uncertainty. It is important to make sure that the different sources of uncertainty are identified when using CMIP models to conduct climate projection. Different responses to the same forcing can emerge due to different processes and feedbacks as well as due to the parameterization used in

the different models (Zelinka *et al.*, 2020). In addition, there are uncertainties existing in the interpolation for outputs from CMIP models to the grid of the observation data with $0.5 \times 0.5^\circ$ through bilinear interpolation. The authors recommend further evaluation of precipitation projections either with more ensemble members, more models or dynamical downscaling with regional models.

ACKNOWLEDGEMENTS

This work was funded by National Key R&D Program of China (2016YFA0602703), the Strategic Priority Research Program of Chinese Academy of Sciences (XDA20060401), the China Postdoctoral Science Foundation (2020M672942), the Fundamental Research Funds for the Central Universities from Sun Yat-Sen University (19lgpy31). We express sincere gratitude to the reviewers for their constructive comments and suggestions. Their advices will benefit the improvement of the article and our future researches.

AUTHOR CONTRIBUTIONS

Xian Zhu: Data curation; formal analysis; methodology; visualization; writing-original draft; writing-review & editing. **Zhenming Ji:** Data curation; formal analysis; investigation; methodology; writing-original draft. **Xiaohang Wen:** Data curation; formal analysis; methodology; software; writing-original draft; writing-review & editing. **Shao-Yi Lee:** Data curation; visualization; writing-original draft; writing-review & editing. **Zhigang Wei:** Investigation; supervision. **Zhiyuan Zheng:** Data curation; visualization. **Wenjie Dong:** Conceptualization; funding acquisition; project administration; resources; supervision; writing-original draft; writing-review & editing.

ORCID

Xian Zhu  <https://orcid.org/0000-0002-5639-6839>

Zhigang Wei  <https://orcid.org/0000-0003-0938-8489>

REFERENCES

- Bao, J. and Feng, J. (2016) Intercomparison of CMIP5 simulations of summer precipitation, evaporation, and water vapor transport over Yellow and Yangze River basins. *Theoretical and Applied Climatology*, 123, 437–452.
- Bao, J., Feng, J. and Wang, Y. (2015) Dynamical downscaling simulation and future projection of precipitation over China. *Journal of Geophysical Research: Atmospheres*, 120, 8227–8243.
- Chen, W., Jiang, Z. and Li, L. (2011) Probabilistic projections of climate change over China under the SRES A1B scenario using 28 AOGCMs. *Journal of Climate*, 24(17), 4741–4756.
- Frich, P., Alexander, L.V., Della-Marta, P., Gleason, B., Haylock, M., Klein Tank, A.M.G. and Peterson, T. (2002) Observed coherent changes in climatic extremes during the

- second half of the twentieth century. *Climate Research*, 19, 193–212.
- Ge, Q.S., Wang, F. and Luterbacher, J. (2013) Improved estimation of mean warming trend of China from 1951–2010 based on satellite observed land-use data. *Climate Change*, 121, 365–379.
- Haarsma, R.J., Roberts, M.J., Vidale, P.L., Senior, C.A., Bellucci, A., Bao, Q., Chang, P., Corti, S., Fuckar, N.S., Guemas, V., von Hardenberg, J., Hazeleger, W., Kodama, C., Koenigk, T., Leung, L.R., Lu, J., Luo, J.-J., Mao, J., Mizielinski, M.S., Mizuta, R., Nobre, P., Satoh, M., Scoccimarro, E., Semmler, T., Small, J. and von Storch, J.-S. (2016) High-Resolution Model Intercomparison Project (HighResMIP v1.0) for CMIP6. *Geoscientific Model Development*, 9, 4185–4208.
- Jin, K., Wang, F., Chen, D., Jiao, Q., Xia, L., Fleskens, L. and Mu, X. (2015) Assessment of urban effect on observed warming trends during 1955–2012 over China: a case of 45 cities. *Climatic Change*, 132, 631–643.
- Kurane, I. (2010) The effect of global warming on infectious diseases. *Osong Public Health and Research Perspectives*, 1(1), 4–9.
- Li, Y., Liu, Y., Ye, W.T., Xu, L.M., Zhu, G.R., Zhang, X.Z. and Zhang, C.Q. (2018) A new assessment of modern climate change, China—an approach based on paleo-climate. *Earth-Science Reviews*, 177, 458–477.
- Mudryk, L., Santolaria-Otín, M., Krinner, G., Ménégoz, M., Derksen, C., Brutel-Vuilmet, C., Brady, M. and Essery, R. (2020) Historical Northern Hemisphere snow cover trends and projected changes in the CMIP6 multi-model ensemble. *Cryosphere*, 14, 2495–2514.
- Omer, A., Ma, Z.G., Zheng, Z.Y. and Saleem, F. (2020) Natural and anthropogenic influences on the recent droughts in Yellow River Basin, China. *Science of the Total Environment*, 704, 135428. <https://doi.org/10.1016/j.scitotenv.2019.135428>.
- Peng, X., She, Q., Long, L., Liu, M., Xu, Q., Zhang, J. and Xiang, W. (2017) Long-term trend in ground-based air temperature and its responses to atmospheric circulation and anthropogenic activity in the Yangtze River Delta, China. *Atmospheric Research*, 195, 20–30.
- Piao, S.L., Ciais, P., Huang, Y., Shen, Z.H., Peng, S.S., Li, J.S., Zhou, L.P., Liu, H.Y., Ding, Y.H., Pingale, S.M., Khare, D., Jat, M.K. and Adamowski, J. (2014) Spatial and temporal trends of mean and extreme rainfall and temperature for the 33 urban centers of the arid and semi-arid state of Rajasthan, India. *Atmospheric Research*, 138, 73–90.
- Shi, Y., Wang, G.L. and Gao, X.J. (2017) Role of resolution in regional climate change projections over China. *Climate Dynamics*, 51, 2375–2396.
- Su, C. and Chen, X. (2019) Covariates for nonstationary modeling of extreme precipitation in the Pearl River basin, China. *Atmospheric Research*, 229, 224–239.
- Sun, Q., Miao, C. and Duan, Q. (2015) Projected changes in temperature and precipitation in ten river basins over China in 21st century. *International Journal of Climatology*, 35, 1125–1141.
- Tang, Y., Guo, Q., Su, C. and Chen, X. (2017) Flooding in delta areas under changing climate: response of design flood level to non-stationarity in both inflow floods and high tides in south China. *Water*, 9, 471. <https://doi.org/10.3390/w9070471>.
- Taylor, K.E. (2001) Summarizing multiple aspects of model performance in a single diagram. *Journal of Geophysical Research*, 106(D7), 7183–7192.
- Taylor, K.E., Stouffer, R.J. and Meehl, G.A. (2012) An overview of CMIP5 and the experiment design. *Bulletin of the American Meteorological Society*, 93, 485–498.
- Tian, Q., Prange, M. and Merkel, U. (2016) Precipitation and temperature changes in the major Chinese river basins during 1957–2013 and links to sea surface temperature. *Journal of Hydrology*, 536, 208–221.
- Tokarska, K.B., Stolpe, M.B., Sippel, S., Fischer, E.M., Smith, C.J., Lehner, F. and Knutti, R. (2020) Past warming trend constrains future warming in CMIP6 models. *Science Advances*, 6, eaaz9549.
- Wang, L., Chen, Y., Niu, Y., Salazar, G. and Gon, W. (2017) Analysis of atmospheric turbidity in clear skies at Wuhan, central China. *Journal of Earth Science*, 28(4), 729–738.
- Wang, R., Zhong, C., Lai, Z., Zeng, Y. and Lian, X.B. (2018) Climate change enhances the severity and variability of drought in the Pearl River basin in south China in the 21st century. *Agricultural and Forest Meteorology*, 249, 149–162.
- Wu, J. and Gao, X.J. (2013) A gridded daily observation dataset over China region and comparison with the other datasets. *Chin. J. Geophys*, 56(4), 1102–1111.
- Wu, J., Liu, Z., Yao, H., Chen, X., Chen, X., Zheng, Y. and He, Y. (2018) Impacts of reservoir operations on multi-scale correlations between hydrological drought and meteorological drought. *Journal of Hydrology*, 563, 726–736.
- Xi, Y., Miao, C.Y., Wu, J.W., Duan, Q.Y., Lei, X.H. and Li, H. (2018) Spatiotemporal changes in extreme temperature and precipitation events in the Three-Rivers Headwater region, China. *Journal of Geophysical Research: Atmospheres*, 123(11), 5827–5844.
- Xin, X., Wu, T., Zhang, J., Yao, J. and Fang, Y. (2020) Comparison of CMIP6 and CMIP5 simulations of precipitation in China and the East Asian summer monsoon. *International Journal of Climatology*, 40, 6590–6440.
- Xu, K., Xu, B., Ju, J., Wu, C. and Hu, B. (2019) Projection and uncertainty of precipitation extremes in the CMIP5 multimodel ensembles over nine major basins in China. *Atmospheric Research*, 226, 122–137.
- Xu, Y., Gao, X.J., Shen, Y., Xu, C.H., Shi, Y. and Giorgi, F. (2009) A daily temperature dataset over China and its application in validating a RCM simulation. *Advances in Atmospheric Sciences*, 26 (4), 763–772.
- Yang, S.L., Xu, K.H., Milliman, J.D., Yang, H.F. and Wu, C.S. (2015) Decline of Yangtze River water and sediment discharge: Impact from natural and anthropogenic changes. *Scientific Reports*, 5 (1). <http://dx.doi.org/10.1038/srep12581>.
- Yu, M., Li, Q., Hayes, M.J., Svoboda, M.D. and Heim, R.R. (2014) Are droughts becoming more frequent or severe in China based on the standardized precipitation evapotranspiration index: 1951–2010? *International Journal of Climatology*, 34(3), 545–558.
- Zelinka, M.D., Myers, T.A., McCoy, D.T., Po-Chedley, S., Caldwell, P.M., Ceppi, P., Klein, S.A. and Taylor, K.E. (2020) Causes of higher climate sensitivity in CMIP6 models. *Geophysical Research Letters*, 47, 1–12.

- Zhang, W., Villarini, G., Scoccimarro, E., Roberts, M., Vidale, P.L., Vanniere, B., Caron, L.-P., Putrasahan, D., Roberts, C., Senan, R. and Moine, M.-P. (2021) Tropical cyclone precipitation in the HighResMIP atmosphere-only experiments of the PRIMAVERA Project. *Climate Dynamics*, <http://dx.doi.org/10.1007/s00382-021-05707-x>.
- Zhao, Q.L., Liu, X.L., Ditmar, P., Siemes, C., Revtova, E., Hashemi-Farahani, H. and Klees, R. (2011) Water storage variations of the Yangtze, Yellow, and Zhujiang river basins derived from the DEOS Mass Transport (DMT-1) model. *Science China Earth Sciences*, 54 (5), 667–677. <http://dx.doi.org/10.1007/s11430-010-4096-7>.
- Zhu, H.H., Jiang, Z.H., Li, J., Li, W., Sun, C. and Li, L. (2020) Does CMIP6 inspire more confidence in simulating climate

extremes over China? *Advances in Atmospheric Sciences*, 37, 1119–1132.

How to cite this article: Zhu, X., Ji, Z., Wen, X., Lee, S.-Y., Wei, Z., Zheng, Z., & Dong, W. (2021). Historical and projected climate change over three major river basins in China from Fifth and Sixth Coupled Model Intercomparison Project models. *International Journal of Climatology*, 1–19. <https://doi.org/10.1002/joc.7206>